Journal of Materials Chemistry A

Accepted Manuscript

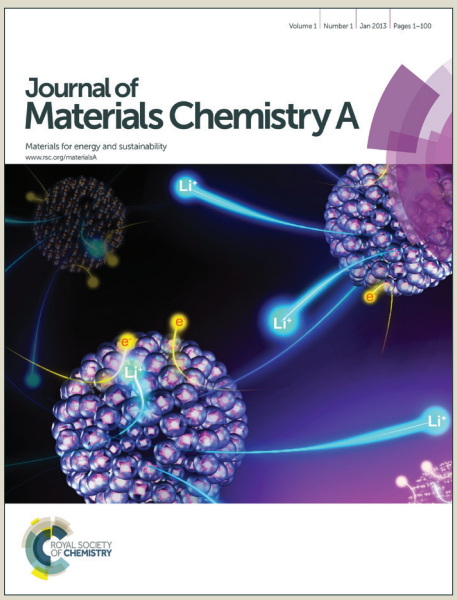

ROYAL SOCIETY OF CHEMISTRY

www.rsc.org/materialsA

Table of contents entry

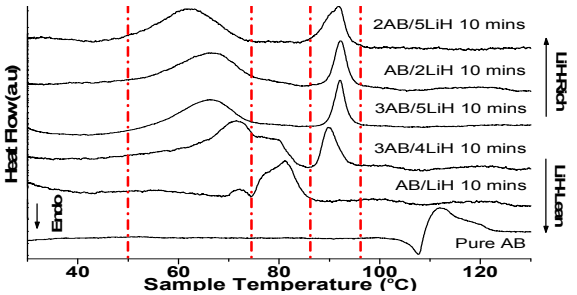

Low energy mixing and higher LiH content effectively destabilizes AB for enhanced hydrogen release at a desirable temperature

Journal Name

RSCPublishing

ARTICLE

Enhanced hydrogen desorption of an ammonia borane and lithium hydride system through synthesised intermediate compounds

Cite this: DOI: 10.1039/xoxxoooooox

Received ooth January 2012,
Accepted ooth January 2012

DOI: 10.1039/xoxxoooooox

www.rsc.org/

Yiwen Wang and Z. X. Guo *

A new hydrogen "storage" strategy is demonstrated for an ammonia borane (AB) and LiH system by means of moderate mechanical milling of the two species under an inert atmosphere. This not only avoids reactive hydrogen release during milling but also leads to formation of intermediate composite $Li_XNH_{3-X}BH_3$ (x<1) to store hydrogen with good stability at ambient temperature. The presence of the intermediate composite and sufficient dispersion of the AB and LiH particles facilitate further reaction of AB and LiH with hydrogen release at a relative low temperature. Herein, we report that the composite system obtained by this simple but effective approach to destabilize AB for enhanced hydrogen release at a desirable temperature. A 10-min milled 3AB/5LiH can release hydrogen of ~ 5.3 wt% at 70 ºC, and another ~ 5.5 wt% at 92 ºC; so a total of ~ 10.8 wt% hydrogen can be obtained before 92 ºC. With an increase of the LiH content, this temperature can be further reduced down to 61 ºC, which is a significant improvement that has not been reported before. Moreover, our results show a much lower dehydrogenation temperature, reduced from 92 to 67 ºC, and a fast kinetics, e.g., 5 and 9 wt% mass loss at 95 ºC within 415 and 1050 s, respectively, which is 6 times faster than reported in the literature (5 and 9 wt% of mass loss at 100 ºC within 2400 and 6900s, respectively). To the best of our knowledge, our system possesses the highest dehydrogenation capacity (5 wt%) at the low hydrogen release temperature (67 ºC), with great improvement on the dehydrogenation kinetics in the solid-state hydride systems. A systemic investigation on the mechanism of the reaction at different milling condition, reaction temperature and LiH content is reported here for the first time.

1. Introduction

Hydrogen has been under intensive investigation as an alternative energy carrier for clean and efficient power supply. However, developing a reliable and economical hydrogen storage system remains one of the most challenge issues [1]. Such a system must satisfy several criteria, such as high storage capacity, safety, low operation temperature, reversibility and low cost.

Ammonia borane, NH_3BH_3 (AB), is one of the promising solid state hydrogen storage materials due to its high gravimetric capacity of 19% and reasonable hydrogen release kinetics under mild conditions [2]. AB exhibits dihydrogen bonding interactions that affect its structure and dynamics [3]. It contains both hydridic B-H and protic N-H bonds that lead to facile hydrogen release through the intermolecular electrostatic interaction between $H^{\delta+}$ and $H^{\delta-}$ on adjacent molecules. Meanwhile, the B-N bond is adequately strong to prevent ammonia and borane emission prior to hydrogen release. A previous study demonstrates that the intramolecular activation barrier for H_2 release is in the range of 134-138 kJ mol^{-1}, which is large than the B-N bond dissociation energy of 108.4 kJ mol^{-1}; this indicates that AB should dissociate to BH_3 and NH_3 before H_2 release [4]. However, the intermolecular AB-AB reaction with subsequent formation of diammoniate of diborane (DADB) leads to a smaller H_2 release energy barrier of ~ 88 kJ mol^{-1}[4]. This may be attributed to intermolecular interaction between $H^{\delta+}$ and $H^{\delta-}$ on adjacent molecules, $H^{\delta+}+H^{\delta-}\rightarrow H_2$, such reaction is energetically favourable to occur. Therefore, hydrogen release from AB is more

favourable than dissociation to ammonia and diborane under most thermolysis conditions [5]. *In-situ* NMR study indicates that the thermal decomposition of AB involving the formation of DADB from the AB-AB interaction, which has more reactive N-H and/or B-H bonds than AB [6]. However the practical application of AB is still restricted by the insufficient hydrogen release kinetics under 100 ºC and the release of other volatile gas products, such as the borazine $B_3N_3H_6$ and diborane (B_2H_6), which could poison the fuel cell. Furthermore, the exothermic nature of the hydrogen release reduces energy efficiency of regeneration of the spent fuel. In the case of thermal decomposition of AB, the reaction enthalpy for H_2 release is reported as ΔH = - 21 kJ mol^{-1} AB [2].

Many approaches have been employed to reduce further the hydrogen release temperature down to 80 ºC, where a PEM fuel cell operates most efficiently, and also to suppress other volatile gas products, and to enhance the decomposition kinetics at mild conditions. For AB, such efforts typically include solvolysis in the presence of an acid [7] or a metal catalyst [8]; acid-catalysed dehydrogenation [9]; and catalytic dehydrogenation by means of transition metal catalysts [10]. Although above approaches show fast kinetics and low temperature for hydrogen release, the formation of thermodynamically stable B-O bonds in spent fuel results in more challenges for regeneration. There are several studies on the thermolysis of AB at both the solid [11] and the solution states [12] in the presence of additives, catalysts and further treatments, i.e. to tailor nanophase structure using nanoporous scaffolds [13], and chemical activation through partial substitution of the protonic hydrogen in the NH_3 group of the AB by a stronger electron-donating element to form metal amidoboranes [14]. In general, thermolysis approaches avoid the formation of B-O and facilitate the regeneration of spent fuel. However, no single approach fulfils all the requirements of the current practical target simultaneously.

Among the above approaches, metal amidoboranes are of particular interest, due to their superior dehydrogenation properties and reduced exothermic heat for system management and easy handing during operation. The approach is based on the substitution of the protonic hydrogen in the NH_3 group of AB by a more electron-donating alkali element. Introduction of an alkali metal leads to the formation of ionic compounds, i.e., alkali amidoboranes (MNH_2BH_3, M = Li and Na). As the alkali metals are a stronger electron-donator than the proton Lewis acid H^+, so N on the $–NH_3$ attracts more electrons directly from the alkali metal rather than H^+, and the H on N becomes less charged with concomitantly more negatively charged H on B. This enhances the activity and the polarity of the $[NH_2BH_3]^-$ ions and changes the chemical bonding of B–N, B–H and N–H, and results in a favourable local combination of $H^{\delta+}$ and $H^{\delta-}$, which has a substantially high chemical potential and then produces H_2 more readily [15]. Thus, alkali metal hydrides adopted here destabilize the dehydrogenation process of AB, introducing a low energy barrier in the hydrogen release pathway. Different alkali amidoboranes have been reported, i.e., $LiNH_2BH_3$ [16], $NaNH_2BH_3$ [17] and $Ca(NH_2BH_3)_2$[18], and various treatments were employed, i.e., in a THF solution [19], mesoporous carbon framework [20]. All these technical advances demonstrate considerable improvements on the dehydrogenation characteristics for both of the extent and kinetics of hydrogen release.

Further investigations show that $LiNH_2BH_3$ can be formed without reported yield through a stepwise reaction between LiH and AB during ball milling, where the $LiNH_2BH_3{\cdot}NH_3BH_3$ is the intermediate of the reaction; a phase transition between α-LiAB and β-LiAB during ball milling is also reported [21, 22]. Recent theoretical and experimental studies on the reaction mechanism of dehydrogenation of alkali and alkaline-earth metal amidoboranes revealed that the dehydrogenation of MAB (M=K, Li, Na) was via a more favourable bimolecular mechanism rather than a unimolecular pathway [23, 24, 25, 26, 27]. The metal atom plays a significantly catalytic role to assist hydride transfer, via the interruption of metal-nitrogen and boron-hydrogen bond to form a metal hydride as an intermediate towards the dehydrogenation. A compound MN(R) =BHN(R) MBH_3 (M=Li or Na, R=H) is concluded as spent fuel after decomposition of metal amidoboranes [26].

More recently, a series of compounds, named ammoniates of amidoborane, have been synthesized through a straightforward method of absorption of NH_3 by related metal amidoborane [28], or alternatively, by mechanical milling AB with related metal amide [29, 30] and imide [31]. $LiNH_2BH_3{\cdot}NH_3$ [28, 29] and $Ca(NH_2BH_3)_2{\cdot}2NH_3$ [30] were reported. However, the thermal decomposition route of such compounds strongly depends on the reaction conditions, an open system with NH_3 vapour pressure close to zero can easily lead to a de-ammoniation of the ammoniate. In contrast, H_2 instead of NH_3 will be predominantly released during the decomposition of ammoniate in a sealed reactor [27]. Some other composite systems, such as mechanically milled $AB/LiNH_2/LiBH_4$ [32] and $LiAB/LiBH_4$ [33] are also developed and investigated. Among them, $AB/LiNH_2/LiBH_4$ mixture in a 1:1:1 molar ratio resulted in the formation of $LiNH_2BH_3$(LiAB) and new crystalline phase(s), the decomposition of this $Li_{2-x}(NH_3)(NH_2BH_3)_{1-x}(BH_4)$/xLiAB composite ($0 < x < 1$) can yield high purity of H_2 at moderate temperatures, it is believed that the favourable dehydrogenation kinetics and suppression of NH_3 evolution result from the coexistence of NH_3 ligand and $LiBH_4$ component [33].

In this study, we are focusing on metal amidoboranes, although it has been intensively studied based on the purpose of the formation of alkali amidoboranes using stoichiometric molar ratio of AB:LiH=1:1; There is no systemic investigation on possible non-stoichiometric AB+LiH composites, where LiH is lean or in excess. It is also unclear about the effects of milling conditions, particularly with a short period of milling/mixing and low energy input. Different milling conditions may lead to the formation of various intermediate compounds during milling and hence subsequent decomposition products. Different intermediate compounds may exhibit various hydrogen release pathways and mechanisms. Moreover, the dehydrogenation properties of the AB/LiH system needs to be improved in order to meet the practical requirements of PEM fuel cells. The dehydrogenation temperature (~ 92 ºC) needs to be further reduced, while the hydrogen release kinetics has to be enhanced. All the issues prompt us to carry out an in-depth investigation on the system. First, we investigate AB mixed with a range of LiH concentrations and different milling conditions. Different milling strategies were employed here in order to disperse sufficiently LiH and AB. An intermediate composite, $Li_XNH_{3-X}BH_3$ ($x<1$) was observed, which facilitates further reaction at a relative low temperature.

2. Experimental

Ammonia Borane (97% purity) was purchased from sigma-aldrich and LiH (98% purity) from Alfa Aesar, both are in powder form of size over micrometres. LiH was pre-milled in a high energy SPEX 8000 mill for 20 hours in order to reduce the particle size and this time was selected from past experience. The SPEX 8000 Mill

shake containers back and forth approximately 1080 cycles per minute (60 Hz model). The typical composition of milling vial and balls are Fe and Cr, with minor elements of Ni, Mn, S and Si. The samples were continuously milled for the pre-set period of time if it was less than 30 mins. Longer milling more than 30 mins was carried out with a pause of 30 mins after every 30 mins, to avoid excessive temperature rise in the sample. A cooling fan was used, when necessary, to maintain the temperature around the milling vial at 30 ^{o}C. Then the LiH powder was mechanically mixed with AB using small milling balls (5 mm in diameter, 0.52 g) in the SPEX mill for different periods of time (5 to 120 mins), and molar ratios of AB:LiH were selected as 1, 3/4, 3/5, 1/2, and 2/5, with corresponding weight ratio as 80/20, 75/25, 70/30, 65/35 and 60/40, respectively. The ball to powder ratio was maintained at 10:1, and all the sample was handled in an Ar (99.9999%) filled glove box, where the H_2O/O_2 level are kept below 0.1 ppm.

Thermal decomposition and gas evolution measurements of pure AB and (AB+LiH) mixture were performed using simultaneous Thermogravimetry (TG) / Differential Thermal Analysis (DTA)/ Mass Spectroscopy (MS). All the samples were heated to 200 ºC at a heating rate of 2 ºC min^{-1} under flowing Ar (99.9999%) of 130mL.min^{-1}.

The phase/structure evolutions were examined by X-ray diffraction (XRD) (Cu Kα radiation, λ=1.54056Å), where all the samples were packed in a borosilicate glass capillary in diameter of 0.5 mm and sealed in the glove box under Ar atmosphere. For XRD analysis, the sample was heated to a typical temperature in the TGA at a heating rate of 2 ºC min-1, and then transferred to the glove box and packed in a protective capillary in the glove box before the analysis. In-situ XRD was also carried out during the thermal decomposition of the sample. The top of the capillary was removed under N_2 flow, so capillary with the sample was covered under a N_2 heating jet, to avoid O_2 or H_2O. The heating rate was controlled at the desirable rate as 2 ºC min^{-1}. The experimental setup details used for this in-situ measurement is presented in scheme S1 in the Supplementary Information.

In-situ solid state 7Li and 11B MAS-NMR was carried out in a Bruker AV600 spectrometer at a frequency of 600 MHz, using a 4 mm-MAS probe. All the samples were tightly packed in a 4 mm ZrO_2 rotor in the glove box, with a pinhole on the vessel cap for venting hydrogen, and the rotor ran at 10 kHz and was heated under N_2 atmosphere. The temperature was calibrated by following the chemical shift of the ^{207}Pb in $Pb(NO_3)_2$ as a function of temperature [34]. The ^{11}B chemical shifts were referenced to solid $NaBH_4$ (-41 ppm).

3. Results and Discussion

3.1 Low energy mechanical milling effects on (AB+LiH) systems

Mechanical milling holds significant potential for microstructure modifications of hydrogen storage materials and synthesis of new phases. In most cases, relatively long milling time and a large ball-to-powder weight ratio are applied in order to generate sufficient energy for the above purposes. Such as the experimental approaches mentioned in the previous reports, the AB+LiH mixture in a molar ratio of 1:1 was mechanically milled under H_2 atmosphere for 2 hrs in a planetary mill at 400 rpm, with a ball (10 mm in diameter)-to-powder ratio of 40:1. The ball milling leads to sufficient reaction between the AB and LiH, a new compound, $LiNH_2BH_3$, was successfully synthesised without any detectable residue. On the other hand, mechanical milling introduces powder mixing, where different species are mixed to achieve a uniform mixture. Moreover, properties of the mixture can also be tailored by controlling the milling time, which directly influences the reaction path. Different reaction paths may involve the formation of a variety of intermediate compounds during ball milling and also subsequent thermal decomposition mechanisms.

3.1.1 Thermal decomposition properties

However, all the previous AB/LiH related studies focused on the formation of alkali amidoboranes. There is no systemic investigation on “metastable” (AB+LiH) systems where LiH is unsaturated or in excess, with variable milling conditions. Herein, we studied the milling effects on dehydrogenation properties of AB and AB+LiH, particularly, with a short period of milling time with low energy input.

Mechanical mixing may lead to reaction and mixing of the components. Mechanical mixing was performed for 5, 10, 15, 30, 60 to 120 mins. The recommended molar ratio of AB:LiH=1/1(weight ratio 80/20) is applied here for primary investigation. Thermal decomposition of ball mixed samples was characterized by combined TG/DTA/MS, see Fig 1. Compared to pure AB, the AB/LiH mixtures exhibit single-step decomposition with a relative low mass loss in the first decomposition stage up to ~ 90 ºC and in the whole reaction up to 200 ºC. The DTA peaks show the first-stage decomposition shifts down to 70-92 ºC, and there is no clear DTA peak corresponding to the second-stage reaction at ~ 150 ºC. The mass loss in the latter decomposition stage starts from ~ 100 ºC and continues until ~ 200 ºC, which is much less exothermic and progresses gradually. The MS results confirm that volatile gas products are largely suppressed during the whole reaction except a small amount of NH_3, which is likely due to residual solvents in as-received AB, as NH_3/THF is used in high-yield AB commercial synthesis [35, 36]. The above results indicate that the LiH destabilizes the AB, leading to fast kinetics and a hydrogen capacity of over 13 wt% before 92 ºC, LiH effectively prevents the formation of volatile gases from undesirable reactions, such as the cross-linking and cleavage of the B-N bond [15]. It is also noted that prolonged mechanical milling from 15 to 120mins deteriorates the dehydrogenation properties of the mixtures: the onset hydrogen release temperature increases from ~ 60 to ~ 70 ºC simultaneously with the increase of the milling time from 15 to 120mins. There are exothermic peaks around ~ 80 ºC throughout all the DTA curves of the samples, and one small peak appears at the early stage ~ 70 ºC, when the ball mill time is less than 30 mins. Transition stage occurs at around 15-30 mins, three exothermic peaks present simultaneously. After 30 mins, the DTA peak around 70ºC disappears whereas another peak evolves at 92 ºC. The mass loss evolution is in accord with the DTA results. To further confirm the transition stage at 30 mins, both of the mass losses of the first stage and the whole reaction to 200 ºC tend to decrease until ball milling at 30 mins, where a critical transition takes place. However, the subsequent mass loss turns back to a decreasing trend again for the sample milled for more than 30 mins. The mass loss decreases along

with prolonged milling probably due to partial decomposition of the materials during milling, which results in hydrogen release and mass loss, as substantial pressure builds up inside the milling vessel was found after prolonged ball milling. The transition occurs after ball milling of 30 mins indicates that some reactions may take place.

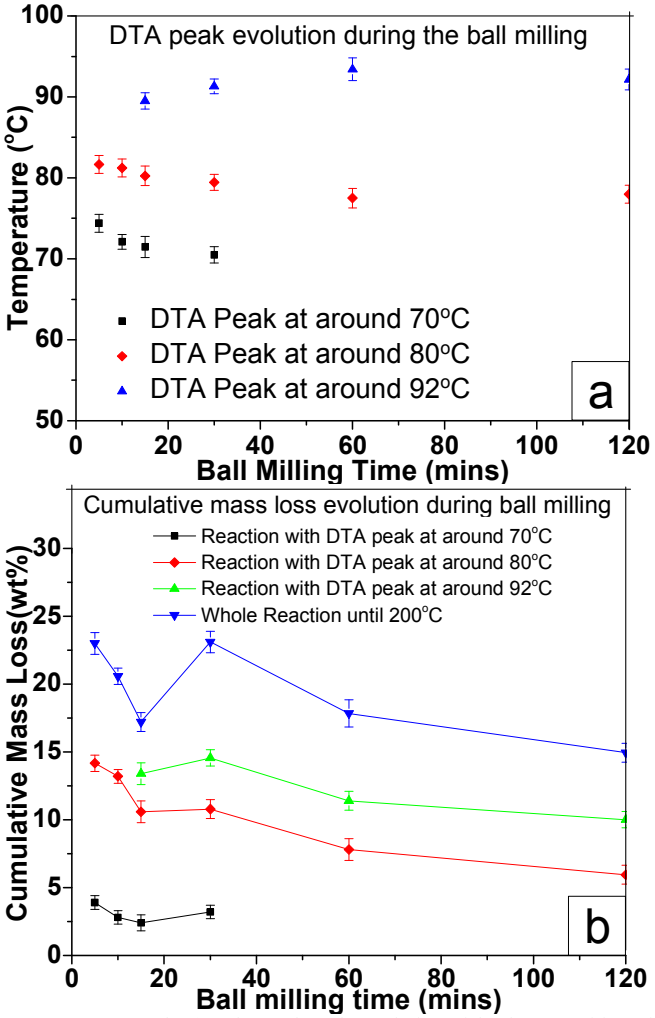

Figure 1 DTA peak (a) and mass loss (b) evolution of the decomposition of AB/LiH as a function of the milling time.

In order to clarify fully the role of LiH and optimize the dehydrogenation conditions, a higher LiH content was introduced into the mixture, and molar ratio of the AB:LiH was selected as 3:5 (weight ratio= 70/30). The higher Li^+ concentration in the system may benefit the B-N bonding and local combination of $H^{\delta+}$ and $H^{\delta-}$, this will be explained more in the latter sections 3.2. The dehydrogenation characteristics of the mixture indeed confirm the assumption. As shown in Fig 2, the higher LiH content leads to further reduction of the hydrogen capacity in the decomposition, but with a lower decomposition temperature. Two main DTA peaks present in most of the samples, which are roughly located at 70 and 92 ºC, except a DTA peak at ~ 80 ºC in the sample milled for 5 mins. The TG and DTA curves for sample milled different periods follow a similar trend: the DTA peak at ~ 70 ºC shifts to a low temperature range with decreased intensity, and finally disappears after milling for 60 mins. While the DTA peak at ~ 90 ºC is more or less unchanged. However, prolonged milling also results in the loss of the hydrogen desorption capacity from the first decomposition, from ~ 7 to ~ 0.6 wt%, whereas almost no change is found in the decomposition at 92 ºC. The result implies that the final hydrogen capacity change may be mainly attributed to the hydrogen capacity loss in the first decomposition step. Furthermore, the 3AB/5LiH mixture exhibits similar mass loss trend to the AB/LiH mixture. The abnormal mass loss increase at ball milling of 30 mins also takes place here; it reveals that this phenomenon is independent on the LiH content of the mixture. In addition, it seems that the 3AB/5LiH mixture ball-mixed for 10 mins shows the best dehydrogenation properties, 5.3 and 10.8 wt% pure hydrogen are obtained at 70 and 92 ºC, respectively.

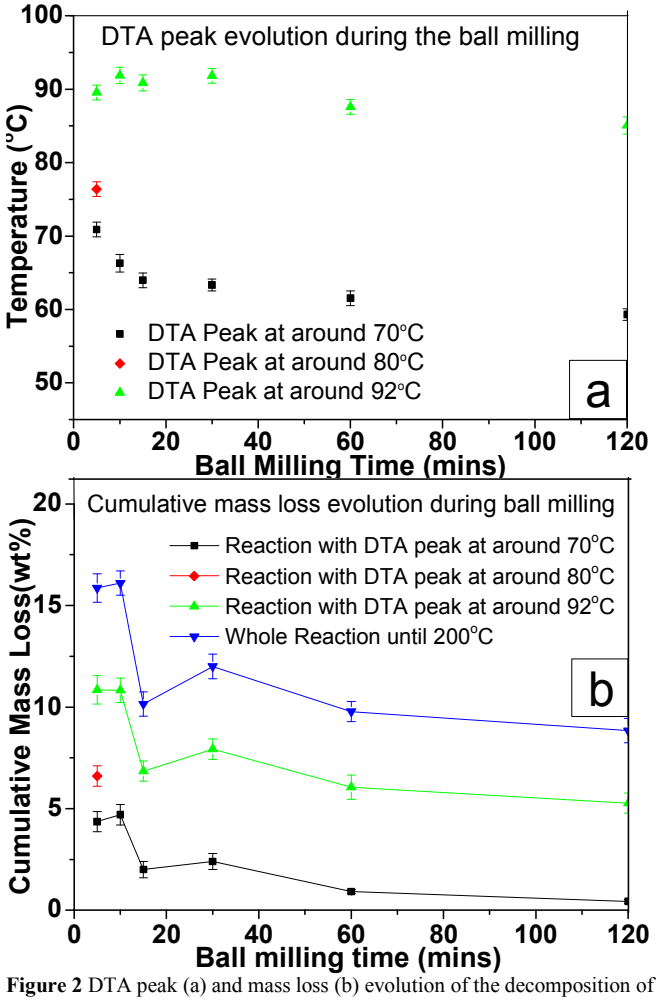

Figure 2 DTA peak (a) and mass loss (b) evolution of the decomposition of 3AB/5LiH as a function of the milling time.

3.1.2 Structural characterisation by XRD

XRD patterns in Fig 3 shows that unreacted AB and LiH still exist in the sample even after ball milling for 60 mins. However, they totally disappear when milling reach 120 mins. While the $LiNH_2BH_3$ and $LiNH_2BH_3{\cdot}NH_3BH_3$ phase that determined by previous reports start to present with a small peak from 10 mins ball milling [22], and its intensity increases significantly with the prolonged ball milling. It is particularly noted that the $LiNH_2BH_3{\cdot}NH_3BH_3$ seems to loose intensity while the $LiNH_2BH_3$ gains intensity when the milling time increases from 60 to 120 mins. It is also noted that one new phase where the peak appears at ca.23º and 28º at 30 mins with rapidly increased intensity, and there are also many weak reflections with increasing milling time. In addition,

the impurity peak in the XRD pattern is originated from contamination of the XRD detector.

It is noted that AB and LiH are still the dominant phases in the sample during the first 30 mins of ball milling, further milling leads to the formation of $LiNH_2BH_3$, $LiNH_2BH_3{\cdot}NH_3BH_3$ and a unknown intermediate phase, as seen in Fig 3. Here, the absence of the DTA peak at ~ 70 ºC and the phase transformation of AB during milling roughly occur after a similar period of milling, 30 mins. Moreover, combined with *in-situ* XRD results for the AB/LiH sample mixed for 10 mins, Fig 5, it is noted that AB reacts with LiH to form completely $LiNH_2BH_3$, $LiNH_2BH_3{\cdot}NH_3BH_3$ and an unknown intermediate phase at ~ 65 ºC. This temperature roughly corresponds to the DTA peak at ~ 70 ºC. Hence, the exothermic reaction at ~ 70 ºC is due to the reaction between AB and LiH. The results clearly show that ball milling can readily induce the reaction of AB and LiH. For a relatively short period of milling, this reaction only progresses to some extent, and the remaining AB and LiH can still react at ~ 70 ºC during subsequent dehydrogenation. Whereas, prolonged milling after 30 mins eventually results in further reaction between AB and LiH, and hence the absence of such a reaction at ~ 70 ºC during dehydrogenation. In other words, the formation of intermediate composite $Li_XNH_{3-X}BH_3$ (x<1) during short and low-energy mixing results in low temperature H_2 release for the 10 min ball milled specimens. This observation has not been noted in previous reports. Increasing milling time increase the peak intensities of $LiNH_2BH_3$, $LiNH_2BH_3{\cdot}NH_3BH_3$, and an unknown intermediate phase. Particularly, $LiNH_2BH_3{\cdot}NH_3BH_3$ partially converts to $LiNH_2BH_3$ when the milling time increases from 60 to 120 mins, which suggests that the formation of $LiNH_2BH_3{\cdot}NH_3BH_3$ here is probably due to insufficient LiH at places, which leads to the reaction of $LiNH_2BH_3$ and AB. However, prolonged ball milling leads to sufficient mixing and reaction of all the species. Further reaction of newly formed $LiNH_2BH_3{\cdot}NH_3BH_3$ with LiH leads to $LiNH_2BH_3$. However, if the LiH content is insufficient and/or cannot be sufficiently dispersed in the system, some $LiNH_2BH_3{\cdot}NH_3BH_3$ still remains in the sample. The overall reactions can be described as follows:

$$LiH + NH_3BH_3 \rightarrow LiNH_2BH_3 + H_2$$

$$LiNH_2BH_3 + NH_3BH_3 \rightarrow LiNH_2BH_3{\cdot}NH_3BH_3, \text{ if locally rich in AB;}$$

$$LiNH_2BH_3{\cdot}NH_3BH_3 + LiH \rightarrow 2LiNH_2BH_3 + H_2, \text{ if locally rich in LiH.}$$

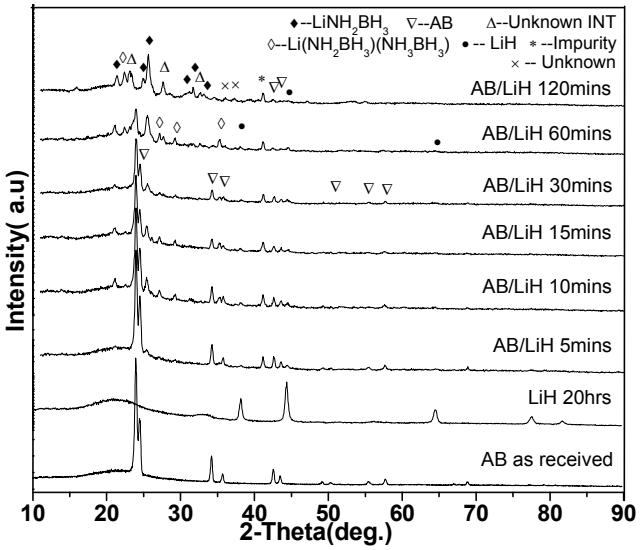

Figure 3 Evolution of XRD patterns of the AB/LiH composition during the ball milling.

XRD patterns in Fig 4 show that a higher LiH content results in rapid formation of $LiNH_2BH_3$, $LiNH_2BH_3{\cdot}NH_3BH_3$ and a new unknown intermediate phase. AB phase cannot be detected after ball milling for 60 mins, while the $LiNH_2BH_3$, $LiNH_2BH_3{\cdot}NH_3BH_3$ and the unknown intermediate phase become dominant. However, prolonged ball milling from 60 to 120 mins leads to a significant phase transformation. The sample after ball milling of 60 mins contains $LiNH_2BH_3$, $LiNH_2BH_3{\cdot}NH_3BH_3$ and an unknown intermediate phase, while the 120 mins ball-milled sample has almost pure and enhanced $LiNH_2BH_3$ phase with a small amount of LiH and some unknown phases. The results indicate that prolonged ball milling leads to further mixing and reaction with hydrogen release; this is consistent with the hydrogen capacity loss in subsequent first thermal-decomposition. And ball milling of 60 mins is sufficient for the complete conversion of AB and LiH. This reaction is more favourable to proceed when the LiH content is higher.

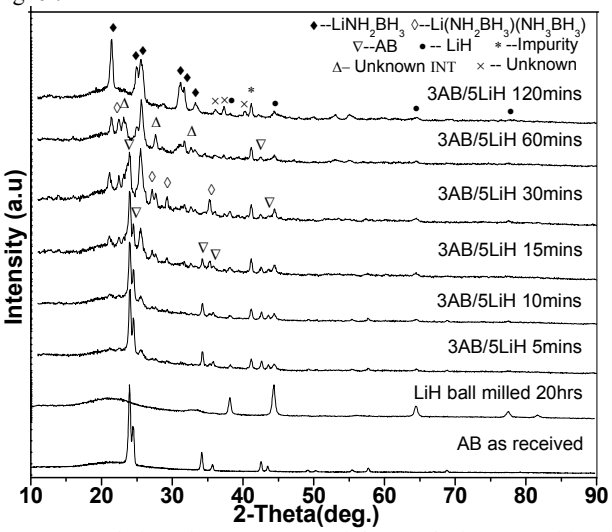

Figure 4 Evolution of XRD patterns of the 3AB/5LiH composition during the ball milling.

In order to determine the contribution of each phase to hydrogen release during the thermal decomposition, our further studies combine the XRD with the TG/DTA results. It is interesting to note

that the sample milled for 120 mins contains almost pure $LiNH_2BH_3$, with only one exothermic peak at ~ 86 ºC in the DTA curve. Furthermore, the mass loss in the temperature range of 80-100 ºC is ~ 5.3 wt %, it roughly matches the theoretical mass loss of 1 mol equiv. of H_2 from the $LiNH_2BH_3$ (5.4 wt %). It strongly implies that this exothermic reaction at ~ 90 ºC should be related to the decomposition of the $LiNH_2BH_3$. Moreover, the sample ball milled for 60 mins contains $LiNH_2BH_3$, $LiNH_2BH_3{\cdot}NH_3BH_3$ and an unknown intermediate phase, and it involves ~ 5.4 wt% hydrogen releases at this decomposition stage. The roughly unchanged hydrogen capacity for these two samples in the decomposition at 80-100 ºC indicates that the $LiNH_2BH_3{\cdot}NH_3BH_3$ may convert to $LiNH_2BH_3$ with slight hydrogen release during further ball milling, due to redundant local LiH content in this LiH-rich samples. While the unknown intermediate phase may undergo decomposition without any gas release or obvious contributes to the mass loss, or phase transition to amorphous. Further combining with the results of the AB/LiH sample ball milled for 120 mins, which contains $LiNH_2BH_3$, $LiNH_2BH_3{\cdot}NH_3BH_3$ and an unknown intermediate phase, and it represents DTA peak at ~ 80 and ~ 90 ºC during thermal decomposition. The insufficient local LiH content in this LiH-lean sample is not favourable for the conversion of $LiNH_2BH_3{\cdot}NH_3BH_3$ to $LiNH_2BH_3$ in the heat treatment. Thus, the newly formed $LiNH_2BH_3{\cdot}NH_3BH_3$ may carry out decomposition rather than conversion to $LiNH_2BH_3$. This suggests that the exothermic reaction at ~ 80 ºC should correspond to the decomposition of $LiNH_2BH_3{\cdot}NH_3BH_3$, and absence of this decomposition in 3AB/5LiH specimens ball milled more than 5 mins is due to the conversion of $LiNH_2BH_3{\cdot}NH_3BH_3$ to $LiNH_2BH_3$ in the locally LiH-rich environment during the further milling. This finding is in agreement with a previous study of the decomposition of $LiNH_2BH_3{\cdot}NH_3BH_3$ [22].

The dehydrogenation temperature of the $LiNH_2BH_3$ observed in this study is roughly in agreement with the temperature in literature (92 ºC) [14]. However, a little lower temperature observed in some of our prolonged milled samples (60 and 120 mins) may be due to a better dispersion of $LiNH_2BH_3$ in the samples; which leads to facile heat absorption and initiation of the decomposition. The lower dehydrogenation temperature of the $LiNH_2BH_3$ observed in 3AB/5LiH mixed for 5 mins is probably due to another mechanism, the insufficient mixing and reaction of AB and LiH during ball mixing leads to non-uniform distribution of LiH, thus the formed $LiNH_2BH_3{\cdot}NH_3BH_3$ undergoes decomposition rather than conversion to $LiNH_2BH_3{\cdot}NH_3BH_3$ in subsequent thermolysis. Both the formation of $LiNH_2BH_3$, $LiNH_2BH_3{\cdot}NH_3BH_3$ and unknown intermediate phase at ~ 70 ºC and subsequent decomposition of $LiNH_2BH_3{\cdot}NH_3BH_3$ at ~ 80 ºC exhibit exothermic feature and generate abundance heat (as shown in the DTA curves in Fig S5), which favours to initiate the dehydrogenation of $LiNH_2BH_3$ at a lower temperature.

It is worth mentioning that the abnormal low mass loss at ~ 70ºC from the 3AB/5LiH sample mixed for 5 mins is probably due to the insufficient mixing of the sample, the insufficient dispersion of the LiH content on AB lead to deficient reaction of LiH and AB with less hydrogen release during the first thermal decomposition at ~ 70ºC. However, subsequent decomposition of the formed $LiNH_2BH_3{\cdot}NH_3BH_3$ provides continued hydrogen release at ~ 80 ºC. The sufficient mixing time over 10mins results in the adequate dispersion, complete reaction of AB with LiH at ~ 70 ºC, and favoured conversion of $LiNH_2BH_3{\cdot}NH_3BH_3$ to $LiNH_2BH_3$, which leads to the absence of the exothermic DTA peak at ~ 80 ºC. The abnormal mass loss change in the sample milled for 30 mins is probably due to the presence of $LiNH_2BH_3{\cdot}NH_3BH_3$ and a new unknown intermediate phase, their decomposition results in more hydrogen release. However, a short period of ball mixing of <15 mins does not lead to sufficient formation of $LiNH_2BH_3$, while prolonged ball milling results in the conversion of $LiNH_2BH_3{\cdot}NH_3BH_3$ to $LiNH_2BH_3$, as a consequence. The total hydrogen capacity in the thermal decomposition of the sample decreases with the increase of milling time.

3.1.3 In-situ XRD and NMR

In-situ XRD and NMR give further insight into the mechanism of hydrogen release pathway of the AB/LiH system through monitoring instant phase evolution and chemical transformation of the sample. As shown in Figs.5 and 6, LiH additive leads to an earlier phase transformation of AB, 60 ºC was observed in the AB/LiH mixture, and much lower temperature at 45 ºC was found in the 3AB/5LiH mixture. The presence of $LiNH_2BH_3$ indicates that AB partially reacts with LiH during ball mixing under current relatively mild conditions. The shift towards to a low-angle and decrease of the intensity of AB are due to unit cell distortion of AB, rupture of dihydrogen bond network, formation of the AB mobile phase and the subsequent reaction of AB with LiH to form $LiNH_2BH_3$ and $LiNH_2BH_3{\cdot}NH_3BH_3$. It is noted that the $LiNH_2BH_3$ and $LiNH_2BH_3{\cdot}NH_3BH_3$ roughly come up simultaneously in both AB/LiH and 3AB/5LiH samples mixed for 10 mins. However, in the former mixture, $LiNH_2BH_3$ reaches maximum intensity at ~ 55 ºC and it subsequently starts to degrade upon further heating in dehydrogenation. While the $LiNH_2BH_3{\cdot}NH_3BH_3$ peaks gradually gain intensity with the increase of temperature. Both $LiNH_2BH_3$ and $LiNH_2BH_3{\cdot}NH_3BH_3$ finally disappear at 75 ºC. The quick phase transformation from crystalline to amorphous at 75 ºC strongly indicates the rapid and intensive decomposition of the sample. The *in-situ* XRD of the latter sample show different characteristics, all of the $LiNH_2BH_3$, $LiNH_2BH_3{\cdot}NH_3BH_3$ and unknown intermediate phase concurrently reach the maximum intensity at ~ 60 ºC, subsequently degrade, and finally disappear at ~ 90 ºC. The degradation of $LiNH_2BH_3$ here is probably due to its decomposition at ~ 90 ºC, whereas the $LiNH_2BH_3{\cdot}NH_3BH_3$ undergoes conversion to $LiNH_2BH_3$ as there is sufficient local LiH particles. The slight peak shifts of the $LiNH_2BH_3$, $LiNH_2BH_3{\cdot}NH_3BH_3$ and the unknown intermediate phases along with the increase of temperature are probably due to the lattice expansion during the heat treatment.

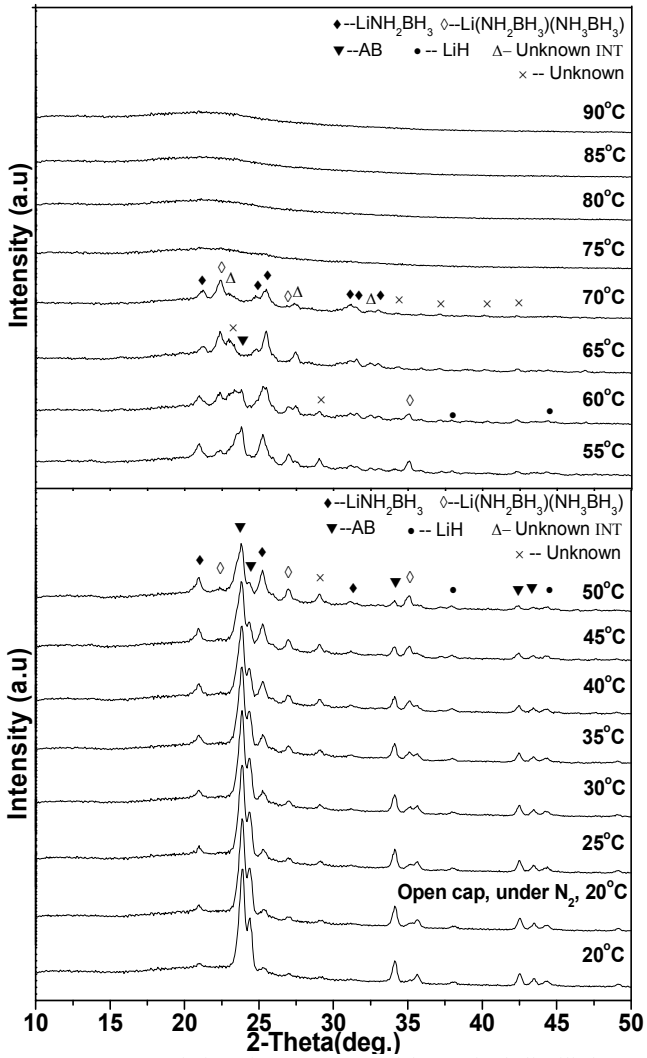

Figure 5 *In-situ* Evolution of XRD patterns of the 10mins ball milled AB/LiH composition during the heat treatment under Ar until 95 ºC, heating rate 2 ºC/min.

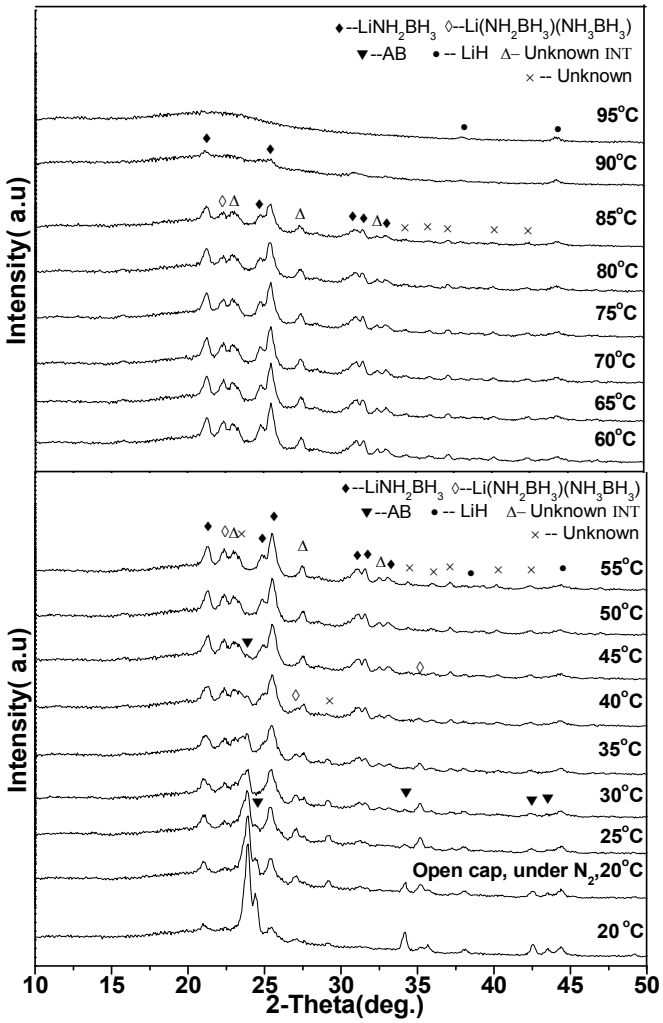

Figure 6 *In-situ* Evolution of XRD patterns of the 10mins ball milled 3AB/5LiH composition during the heat treatment under Ar until 95 ºC, heating rate 2 ºC/min.

In-situ NMR results further explore the evolution of boron and lithium-containing intermediates and products. The results are quite helpful to gain a better understanding of the hydrogen release mechanism. Fig 7 reveals that AB/LiH mixture ball mixed for 10mins contains two borane species with chemical shift of -24.2 and -20.1 ppm, which are consistent with the previously published NMR data of AB and $LiNH_2BH_3$ species [14, 19], the downfield shift of ^{11}B resonance in $LiNH_2BH_3$ complex compared to that in the AB suggests that the lithium amid group $–NH_2(Li)–$ forms a stronger electron donor-acceptor complex with borane, and it leads to a reduction of electron density around borane. It is consistent with the previously observed shortening of the B-N bond in $LiNH_2BH_3$ as well [15]. With the increase of temperature, the ^{11}B resonance of AB degrades, while the peak intensity of the $LiNH_2BH_3$ increases, both of the peaks totally disappear at around 55 and 57 ºC, respectively. Subsequently, one new B specie at δ = -21.8 ppm is observed at 51 ºC, where the transition occurs, three $-BH_3$ species present at same time. After 51 ºC, the intensity of the chemical shift of -21.8 ppm gradually increase until 67 ºC, where another ^{11}B resonance at -22.9 ppm is also observed. Both of these two ^{11}B resonances are associated with the $-BH_3$ species. Combined with the *in-situ* XRD, the complex which contains $-BH_3$ species could be $LiNH_2BH_3{\cdot}NH_3BH_3$ due to the similar temperature range of

presence, as repeated in previous reports [15, 22]. The new ^{11}B resonance at -22.9 ppm could correspond to the unknown compound from the decomposition of $LiNH_2BH_3{\cdot}NH_3BH_3$. It is also noted that there is one weak and quick ^{11}B resonances at -7.7 ppm observed at temperature range of 57 to 65 ºC, which correspond to the BH_2 species. Additionally, a ^{11}B resonance at 29.8 ppm is also found at the similar temperature range, with subsequent evolution of another new ^{11}B resonance at 26.7 ppm from 63 ºC, both of these ^{11}B resonances can be assigned to sp^2 borane in the polyborazylene.

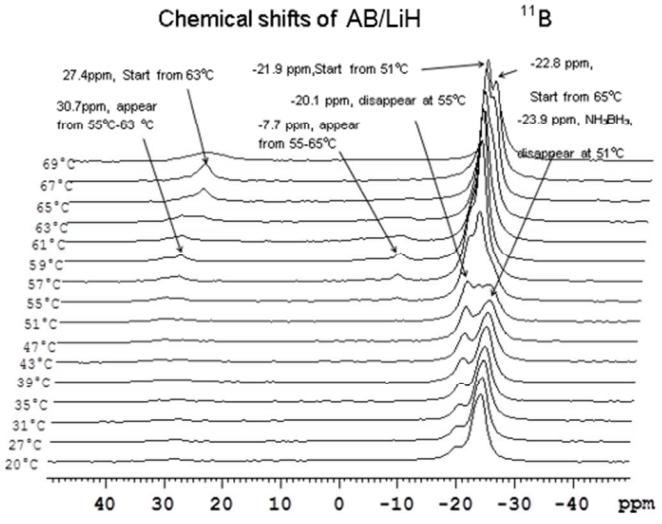

Figure 7(a) *In-situ* ^{11}B MAS NMR spectra of the AB/LiH after dehydrogenation upon 69ºC, heating rate 2 ºC/min. please note: Data collection ends abruptly at around 69ºC as the sample extruded (like toothpaste due to the foaming) out of the rotor while spinning.

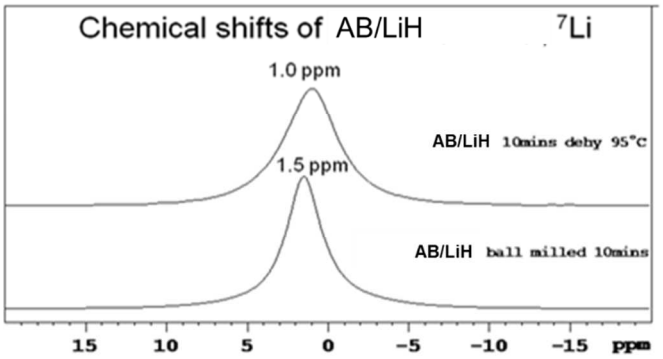

Figure 7(b) ^{7}Li MAS NMR spectra of the AB/LiH after dehydrogenation upon 95ºC, heating rate 2 ºC/min.

The results exhibit the presence of the $LiNH_2BH_3$ in ball mixed sample and early stage of heat treatment until 55 ºC. However, no BH_2, BH_4 species are observed during the thermal decomposition, which implies that diammoniate of doborane is not formed during thermolysis, thus there is no self-decomposition of AB in this sample, unlike the case for pure AB. Furthermore, the $LiNH_2BH_3{\cdot}NH_3BH_3$ complex shows a very close chemical shift (-21.8 ppm) to the AB mobile phase (-22.3 ppm). It is of a higher electron density around B than that of $LiNH_2BH_3$ but lower than that of pure AB. This indicates that this complex may have both dihydrogen bond and ionic bond features. The observation is in agreement with a recent study of this complex, which demonstrates that $LiNH_2BH_3{\cdot}NH_3BH_3$ is composed of alternative $LiNH_2BH_3$ and AB layers [22]. Moreover, $LiNH_2BH_3{\cdot}NH_3BH_3$ shows very similar dehydrogenation products to AB. The presence of BH (N_3) and sp^2 borane after 55 ºC strongly suggests that the dehydrogenation products may be borazine($B_3N_3H_6$)-like or polyborazylene($B_3N_3H_4$)-like compounds, which is consistent with a trigonal planar N-BH-N environment for borane. This indicates that the $LiNH_2BH_3{\cdot}NH_3BH_3$ may undergo cyclotriborazane decomposition to a borazine-like compound and further decomposition to a polyborazylene-like compound. However, we cannot rule out the likelihood of the formation of PAB-like products (polymeric aminoborane (PAB), $(H_2NBH_2)_n$), such as $LiNHBH_2{\cdot}NH_2BH_2$ or $LiNH_2BH{=}NHBH_3$ due to the existence of NMR signals around -22 ppm which is assigned to the terminal $-BH_3$ species. The mechanism of decomposition of $LiNH_2BH_3{\cdot}NH_3BH_3$ has been proposed and reported in the previous reports [21], and it can be described by the followed equation:

$$LiNH_2BH_3{\cdot}NH_3BH_3(s) \rightarrow [LiN_2B_2H_7]\ (s) + 2H_2\ (g) \qquad 80\ ºC$$

$$[LiN_2B_2H_7]\ (s) \rightarrow [LiN_2B_2H]\ (s) + 3H_2\ (g) \qquad 140\ ºC$$

Hence, if this is the case, the $LiN_2B_2H_7$ should possess a borazine-like or a PAB-like structure, while LiN_2B_2H may have a polyborazylene-like structure and exhibit amorphous feature.

Due to sample foaming observed during heat treatment in NMR rotor. The sample of AB/LiH was extruded out of the rotor like toothpaste while spinning and the data collection ended abruptly at around 69 ºC. So it is not recommended to run any more *in-situ* NMR measurement for this sample. Hence, ^{7}Li magic-angle spinning (MAS) NMR measurement was carried out on the post ball-mixed and decomposed samples upon specific temperature of 95 ºC. The result shows that the AB/LiH mixture just ball mixed for 10 mins contains lithium species with a chemical shift of 1.5 ppm, while the dehydrogenation product upon 95 ºC shows a chemical shift with respect to the peak at 1.0 ppm. The upfield shifts is consistent with the dehydrogenation process of the sample, the removal of the hydrogen from N on $LiNH_2BH_3$ or $LiNH_2BH_3{\cdot}NH_3BH_3$, leads to reduction of the electronegativity of N. It results in the increase of electron density on Li.

Fig 8 shows *in-situ* NMR result for the 3AB/5LiH mixture ball mixed for 10 mins. This sample contains borane species with chemical shift of -24.3 and -20.2 ppm, which are consistent with the ^{11}B resonance for the AB and $LiNH_2BH_3$ species. The supersaturated LiH content leads to earlier disappearance of the AB at 51ºC, which is consistent with the results in the *in-situ* XRD. Moreover, $LiNH_2BH_3$ exists from room temperature until 77ºC, where another new ^{11}B resonance at δ = -22.3ppm is observed, which can be assigned to the unknown intermediate complex. This peak graduately looses its intensity and becomes broadened and featureless with the increase of temperature. It slightly shifts downfield to -22.0 ppm until 97 ºC. A new broad peak with chemical shift of 26.4 ppm appears after 67 ºC, and it slightly increases its intensity with the increase of temperature, which should correspond to the sp^2 borane in the polyborazine-like compound. The results of *in-situ* solid state ^{7}Li for the 3AB/5LiH are similar to those of the AB/LiH. The 3AB/5LiH sample mixed for 10 mins contains lithium species with a chemical shift of 1.4 ppm until 77 ºC, and it shifts upfield with respect to the peak at 1.0 ppm after 83 ºC.

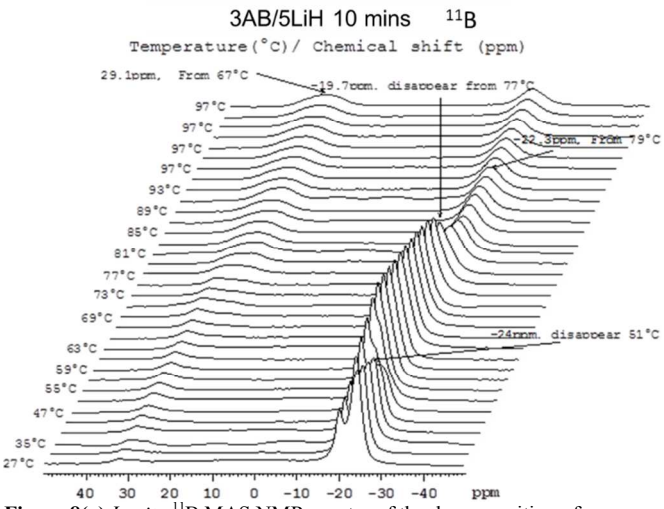

Figure 8(a) *In-situ* ^{11}B MAS NMR spectra of the decomposition of 3AB/5LiH upon 97 °C, heating rate 2 °C/min.

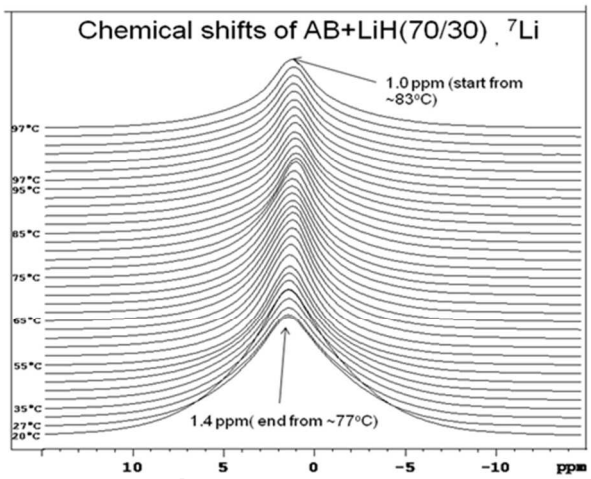

Figure 8(b) *In- situ* ^{7}Li MAS NMR spectra of the decomposition of 3AB/5LiH upon 97 °C, heating rate 2 °C/min.

Hence, as described above, it is clarified that prolonged ball milling deteriorates the dehydrogenation properties of the AB+LiH system. It results in *in-situ* reaction of AB and LiH with concurrent hydrogen release during milling. This pre-reaction is undesirable, and leads to a reduction of hydrogen capacity around 70 ºC during subsequent dehydrogenation. The experiments show that ball-mixing for 10 mins is enough to achieve sufficient mixing of the two components without inducing excessive *in-situ* reaction, leading to optimal dehydrogenation properties: a relative low dehydrogenation temperature from ~ 70 ºC and a high hydrogen capacity of 10.8 wt.% before ~ 92 ºC. Herein, a new hydrogen storage strategy is demonstrated in present study: only using a low-energy milling, eg, small milling balls, short milling time to mix the reactants under an inert atmosphere to avoid further hydrogen release reaction during milling; an intermediate composite $Li_XNH_{3-X}BH_3$ (x<1) can be formed to store hydrogen with good stability at ambient temperature. The presence of an intermediate composite and sufficient dispersion of AB and LiH facilitate subsequent hydrogen release at a relative low temperature during the dehydrogenation stage. The presence of the intermediate composite and sufficient dispersion of the AB and LiH facilitate the further reaction of AB and LiH and hydrogen release at a relative low temperature. Thus, we report that the composite systems which obtained through this simply but effective approach destabilizes AB with promoted hydrogen release at a desired temperature. Such AB+LiH system is ideal for practical applications in powering PEM fuel cells.

3.1.4 Isothermal measurement

The isothermal dehydrogenation of the 3AB/5LiH mixed for 10 mins shows great improvements in dehydrogenation at 75, 85 and 95 ºC, the sample has a higher level of released hydrogen and relatively fast kinetics. In Fig 9 (a), even at 75 ºC, 4.7 wt% H_2 was released within 1300 s. At 85 and 95 ºC, a two-stage dehydrogenation reactions further enhances hydrogen release. Particularly, the dehydrogenation time in the second decomposition stage at 95 ºC is less than half of that at 85 ºC. At 95 ºC, 5 and 9 wt% mass loss are achieved within 415 and 1050 s for the two stages, respectively. Compared to pure $LiNH_2BH_3$ in previous reports, which achieved 5 and 9 wt% of mass loss at 100 ºC within 2400 and 6900 s, respectively [14, 15, 16], the current ball-mixed 3AB/5LiH sample shows great improvement in dehydrogenation kinetics, about 6 times at 95 ºC. The MS profiles at the isothermal measurement are shown in Fig 9 (b). It is corresponding to note that there are no evident NH_3, B_2H_6 and $B_3N_3H_6$ detected during the isothermal dehydrogenation at all the cases. The enhanced dehydrogenation properties in our system are probably due to the facile reaction of AB and LiH at low temperature of ~ 70 ºC, which is exothermic and can provide heat for subsequent dehydrogenation at a higher temperature. Furthermore, the optimized milling conditions play a key role in the evolution of this reaction, prolonged ball milling leads to the reaction of AB and LiH during milling rather than in thermal decomposition, which reduces the overall hydrogen capacity. The *in-situ* XRD measurements in isothermal dehydrogenation at 85 and 75ºC (as shown in Fig S4) indicates that the 3AB/5LiH sample shows similar dehydrogenation pathways at isothermal and scan modes, a much higher heating rate does not alter the reaction route.

Figure 9 (a) Mass loss of dehydrogenation at 75, 85 and 95 ºC under flowing argon for the 10mins ball milled 3AB/5LiH, heating rate at 30 ºC/min.

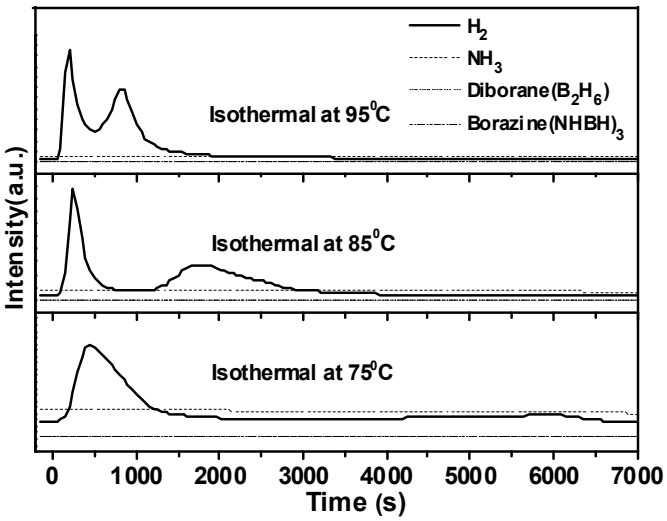

Figure 9 (b) MS profiles of dehydrogenation at 75, 85 and 95 ºC under flowing argon for the 10mins ball milled 3AB/5LiH, heating rate at 30 ºC/min.

3.2 Effect of LiH additive on AB

LiH content plays a very important role in dehydrogenation of the AB system. The introduction of LiH leads to the formation of ionic compounds, i.e., Lithium amidoboranes ($LiNH_2BH_3$). Thus, LiH adopted here destabilizes the dehydrogenation process of AB, introducing a low energy barrier hydrogen release. However, all the previous studies in literature focuses on the formation of alkali amidoboranes, there is no systemic investigation reported for the "metastable" (AB+LiH) systems where the LiH is unsaturated or in excess. Different LiH contents have been tested in our studies under optimized milling conditions.

As shown in Fig. 10, with increase of LiH content from unsaturated to over-saturated, AB:LiH molar ratio from 1/1 to 2/5, the temperature of first decomposition reduces to ~ 60 ºC, and the hydrogen capacity of the whole dehydrogenation decreases as well. Whereas, the hydrogen capacity of the first dehydrogenation stage exhibits parabola feature, it firstly increases and then decreases, the sample 3AB/5LiH has a largest mass loss at the first dehydrogenation stage of ~ 5.3 wt%. However, the mass loss of the first dehydrogenation in LiH-lean and LiH-rich samples may be attributed to different mechanisms. The reduced hydrogen release in the LiH-lean sample may be due to insufficient local LiH for complete reaction of AB and LiH, although 10mins ball mixing may be sufficient to disperse LiH in AB. While the reduced mass loss in the LiH-rich sample may result from the fact that the excess level of LiH favours its *in-situ* reaction with AB during ball mixing and leads to a low H_2 content for subsequent reaction during thermal dehydrogenation.

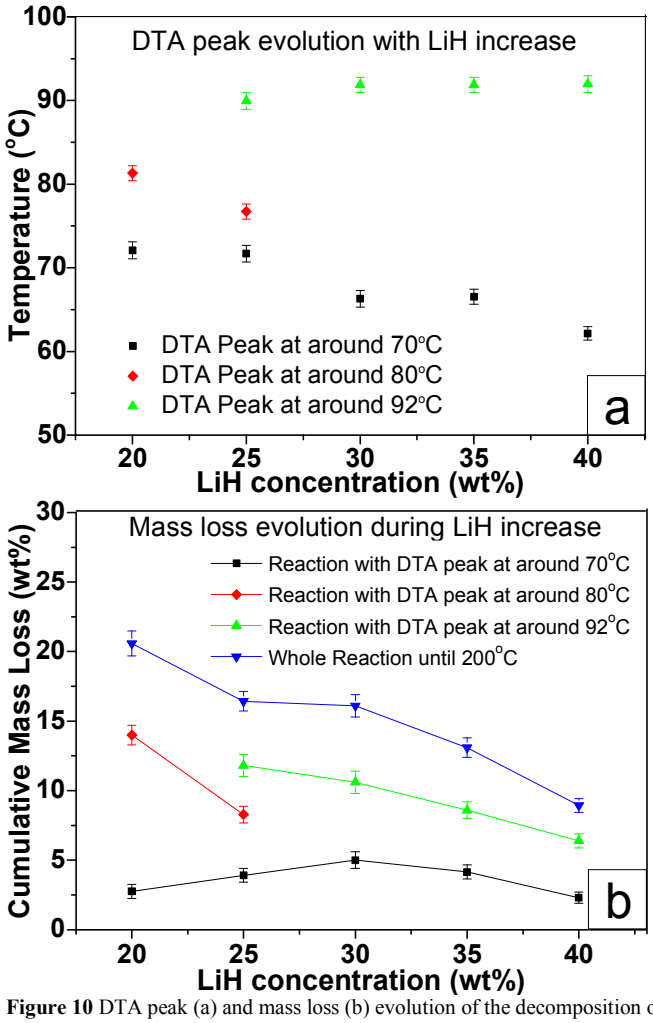

Figure 10 DTA peak (a) and mass loss (b) evolution of the decomposition of AB+LiH composition as a function of the LiH content

In addition, we believe that the increase of the LiH content leads to a different hydrogen release pathway during dehydrogenation. For LiH-lean sample, such as AB/LiH, the dehydrogenation should involve initial reactions of AB and LiH, i.e. the formation of $LiNH_2BH_3$ until 55ºC, and subsequent reaction between $LiNH_2BH_3$ and NH_3BH_3 to form $LiNH_2BH_3{\cdot}NH_3BH_3$ when local LiH content is insufficient, finally, quick stepwise decomposition of $LiNH_2BH_3{\cdot}NH_3BH_3$ to produce borazine-like or polyborazine-like compounds. And these two hydrogen release steps take place more or less concurrently. However, dissimilar pathways represent in LiH-rich sample, such as 3AB/5LiH, the newly formed $LiNH_2BH_3{\cdot}NH_3BH_3$ during mixing and at the early stages of dehydrogenation can be fully converted to $LiNH_2BH_3$ at a higher temperature due to an excess level of LiH. The final hydrogen release is attributed to the decomposition of the $LiNH_2BH_3$. Moreover, $LiNH_2BH_3$ exists from room temperature to 77 ºC, and no $LiNH_2BH_3{\cdot}NH_3BH_3$ is observed before or after the decomposition of $LiNH_2BH_3$, which indicates that a higher LiH content is more favourable for the conversion of $LiNH_2BH_3{\cdot}NH_3BH_3$ to $LiNH_2BH_3$ in the dehydrogenation process. The sp^2 borane and $-BH_3$ species observed after the decomposition of $LiNH_2BH_3$ imply that the decomposition pathway is not as simple as that proposed in the previous report [15]. It is suggested that the $LiNH_2BH_3$ may undergo intermolecular decomposition and produce branched chain-like compounds, rather than linear polymeric products. Such stepwise decomposition may take place very quickly, thus the decomposition

product in the first step can barely be observed in the *in-situ* NMR. Our NMR finding agrees with previous study very well [26]. The actual decomposition products may be a mixture of compounds with different length but should contain both sp^2 borane and $-BH_3$ species. One possible compound with these features is suggested by previous study as MN(R) =BHN(R)MB_3 (M=Li or Na, R=H_2) [26]. Such result is in accord with the computational study on the hydrogen release mechanism of $LiNH_2BH_3$ [23, 24, 25]. The decomposition progress may involve the rate limiting step of breaking of B-H and Li-N to form Li-H-Li complex, followed by the combination of $H^{\delta-}$ on Li and $H^{\delta+}$ on N. The Li ion plays an important role in the reaction to assist hydride transfer. Moreover, the mechanism of hydrogen desorption was revisited by recent studies [33, 34], which indicated that the hydrogen release process is facilitated not only by heteropolar N-H···H-B proton-hydride interactions, but also by homopolar B-H···H-B interactions [37, 38]. The thermolysis of $LiND_2BH_3$ results in the evolution of HD and H_2 with a ratio of approximately 2:1, providing an evidence of a bimolecular reaction pathway, the hydrogen gas is majorly produced through a proton-hydride interaction but with a significant contribution from a hydride-hydride interaction. And such B-H···H-B interactions pathway has been found to extent dramatically at a higher thermolysis temperature, in the case of NH_3BH_3. However, the hydrogen release may not arise directly from the B-H···H-B interactions, it may actually arise indirectly from the Li-H···H-Li or Li-H···H-B interactions, presumably by hydrogen transfer between neighbouring borane moieties. A short B-H···H-B contact in $LiNH_2BH_3$ is believed to facilitate the hydrogen release through this homoplar dihydrogen bonding, a B-H···H-B contact of 2.11 Å in $LiNH_2BH_3$ compares to 3.05 Å in NH_3BH_3 is reported in computational study [37]. Thus, a structure with closer B-H···H-B contact is preferable. The possible reaction route and decomposition products of $LiNH_2BH_3$ are proposed and described in scheme 1. Therefore, the unknown intermediate compounds present during the ball mixing and thermolysis could be the first stage decomposition product of $LiNH_2BH_3$: $LiNH_2BH_2LiNHBH_3$.

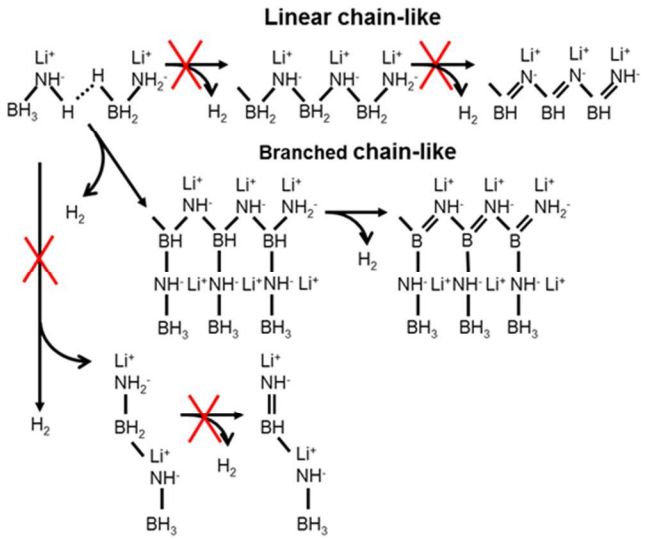

Scheme 1 Proposed reactions and hydrogen release pathways from $LiNH_2BH_3$

It is also noted that LiH strongly suppresses the formation of volatile gas products: There is no evident B_2H_6, $B_3N_3H_6$ and NH_3 from the thermal decomposition of the samples with LiH contents over 30 wt% (3AB/5LiH). It indicates that the substitution of the protonic hydrogen in the NH_3 group of AB by Li leads to a stronger chemical bonding of B-N, and favours hydrogen release during the thermal decomposition. Previous computational study reported the introduction of Li^+ changes the chemical bonding of B–N, B–H and N–H, a shorter B-N bond lengths of ~ 1.547Å in $LiNH_2BH_3$, compared to ~1.58 Å in solid AB, were calculated. [15]. Thus, a higher Li^+ concentration may enhance the activity and the polarity of the $[NH_2BH_3]^-$ ions, and further prevent the breaking of B-N bonding. The introduction of a higher LiH content also leads to the elimination of the second decomposition stage of AB, which is around ~ 145 ºC. Only a certain amount of the hydrogen was released at ~ 130 ºC in the AB/LiH sample. The result implies that the introduction of LiH leads to a totally different dehydrogenation pathway from pure AB. Another benefit of LiH is to trap the residual NH_3 from as-received AB [41]. However, the efficiency of this may not be obvious in the case of LiH-lean sample, as a small trace amount of NH_3 was still detected in AB/LiH sample.

Conclusions

In summary, it is discovered that a short and low-energy mechanical mixing of AB and LiH under an inert atmosphere can lead to a partial reaction of AB and LiH to a desirable extent without excessive hydrogen release during milling. The specific period has been identified as 10 mins using the SPEX 8000 mill. An intermediate composite $Li_XNH_{3-X}BH_3$ (x<1) is formed to store hydrogen with good stability at ambient temperature. The presence of some newly formed $LiNH_2BH_3$ during the initial mixing is favourable for further nucleation of this phase during subsequent dehydrogenation. Sufficient dispersion of AB and LiH facilitates their dehydrogenation reaction at a relative low temperature. This pre-preparation strategy is effective to meet the practical requirements of PEM fuel cells, as sufficient hydrogen (~ 5 wt.%) can be released below 80 ºC with satisfactory kinetics. Moreover, the exothermic feature of the reaction of AB and LiH provides abundant heat to initiate and accelerate the second dehydrogenation reaction. Such mechanism does make the 3AB/5LiH mixtures possess a dehydrogenation kinetics of 6 times faster than others at 95 ºC. The LiH content also plays an important role in the dehydrogenation properties of the (AB+LiH) mixture. Different reaction mechanisms and hydrogen release pathways are observed when the LiH content varies. In contrast to previous reports on the sample of AB/LiH, our study demonstrates that the LiH-rich samples, particular 3AB/5LiH mixed for 10 mins, exhibits better dehydrogenation properties than the LiH-lean samples, i.e., with faster hydrogen release kinetics at a lower temperature.

Comparison of the AB/LiH and the 3AB/5LiH samples under different ball-mixing and thermal-decomposition conditions are schematically shown in Scheme 2. The proposed reaction and decomposition pathways of the samples during ball mixing/milling and dehydrogenation are outlined. Proposed reactions during the accordingly dehydrogenation reactions of the samples with different LiH contents are shown in Scheme 3. Both figures provide a comprehensive picture of the mechanistic pathways for hydrogen release in the solid-state AB+LiH systems.

The dehydrogenation properties of our systems meet the DOE 2015 target and show great potential for the practical application on PEM fuel cell. However, the reactions are very complicated, further study need to be carried out to fully understand the mechanism and maximize the hydrogen capacity at the lower temperature range, also develop energy-efficient regeneration route.

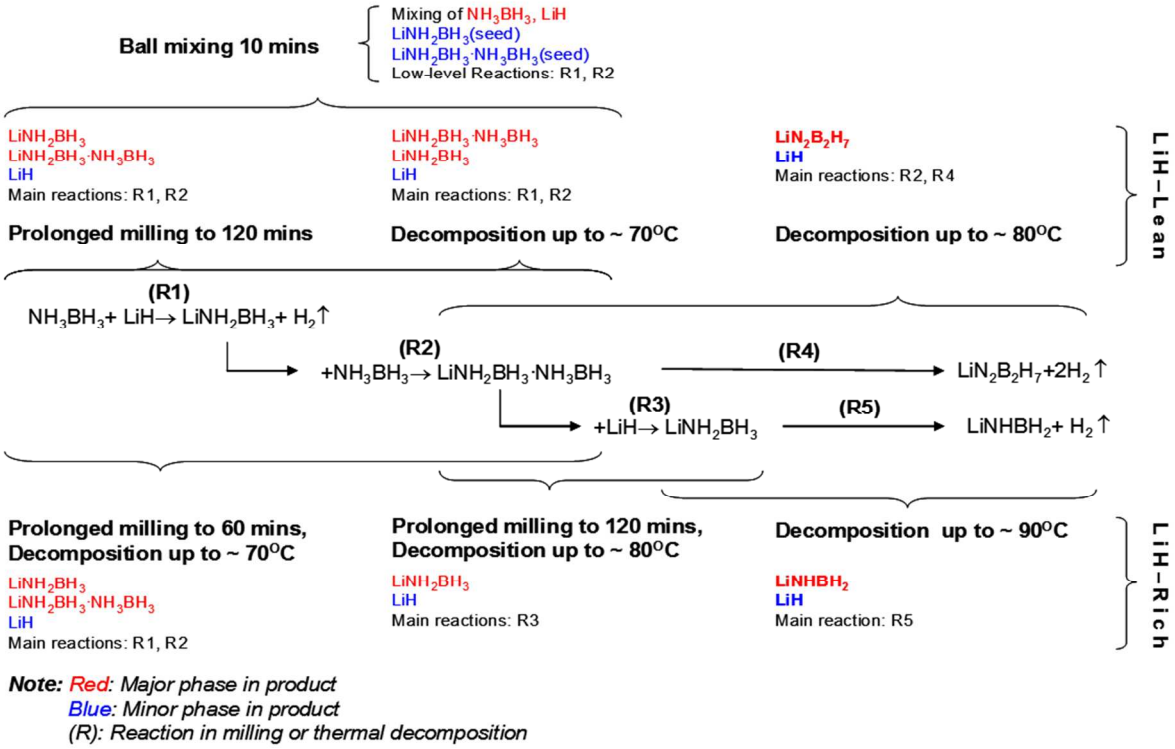

Scheme 2 Proposed main reaction pathways during the thermal decomposition or ball milling of the AB+LiH system with different LiH content

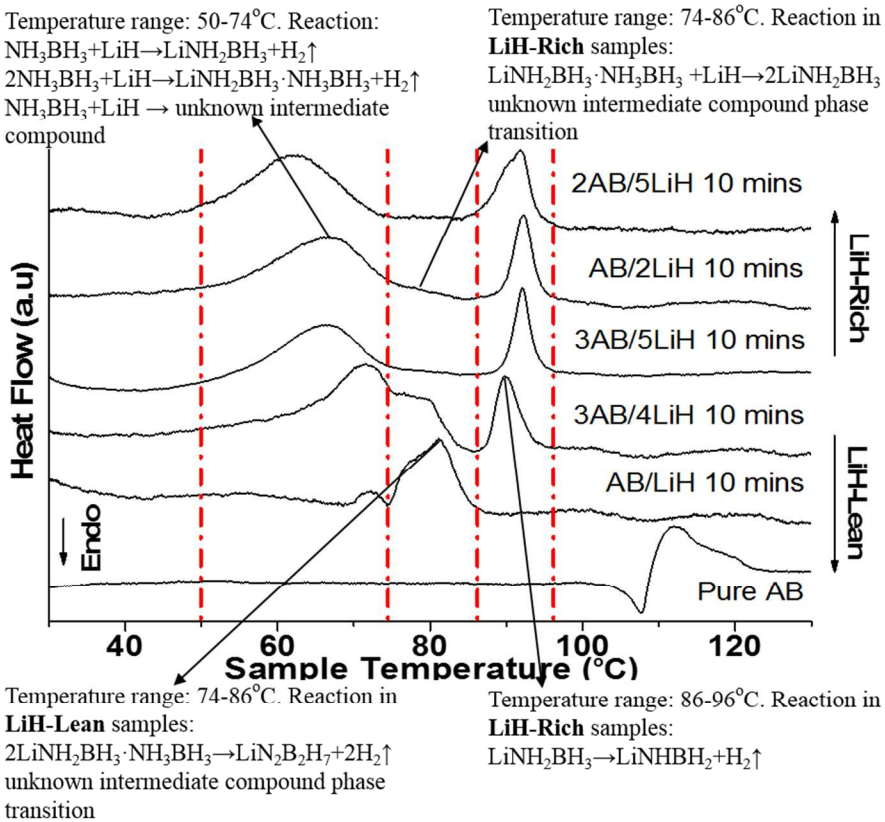

Scheme 3 Proposed reactions and hydrogen release pathways occurring in different temperature ranges for the mixed AB+LiH samples with different LiH content.

Acknowledgements
The project was funded by the UK EPSRC under the SUPERGEN Initiative (Grant No. EP/E040071/1 and EP/K021192/1).

Notes and references
Department of Chemistry, University College London, 20 Gordon Street, WC1H 0AJ, United Kingdom

1 L. Schlapbach and A. Züttel, *Nature*, 2001, **414**, 353-358.
2 G. Wolf, J. Baumann, F. Baitalow and F. P. Hoffmann, *Thermochim. Acta*, 2000, **343**(1-2), 19-25.
3 W. T. Klooster, T. F. Koetzle, P. E. M. Siegbahn, R. B. Richardson and R. H. Crabtree, *J. Am. Chem. Soc.,* 1999. **121**(27), 6337-6343.
4 V. S. Nguyen, M. H. Matus, D. J. Grant, M. T. Nguyen and D. A. Dixon, J. Phys. Chem. A, 2007. **111**(36), 8844–8856.
5 F. H. Stephens, V. Pons and R. T. Baker, *Dalton Trans.,* 2007, **25**, 2613-2626.
6 A. C. Stowe, W. J. Shaw, J. C. Linehan, B. Schmid and T. Autrey, *Phys. Chem. Chem. Phys*., 2007. **9**(15), 1831-1836.
7 G. E. Ryschkewitsch, *J. Am. Chem. Soc*., 1960, **82**(13), 3290-3294.
8 M. Chandra and Q. Xu, *J. Power Sources*, 2006, **156**(2), 190-194.
9 F. H. Stephens, R. T. Baker, M. H. Matus, D. J. Grant and D. A. Dixon, *Angew. Chem. Int. Ed*., 2007, **46**(5), 746-749.
10 C. A. Jaska, K. Temple, A. J. Lough and I. Manners, *J. Am. Chem. Soc.*, 2003, **125**(31), 9424-9434.
11 G. Wolf, J. Baumann, F. Baitalow and F. P. Hoffmann, *Thermochim. Acta*, 2000, **343**(1-2), 19-25.
12 M. E. Bluhm, M. G. Bradley, R. Butterick, U. Kusari and L. G. Sneddon, *J. Am. Chem. Soc.,* 2006, **128**(24), 7748-7749.
13 A. Gutowska, L. Y. Li, Y. S. Shin, C. M. M. Wang, X. H. S. Li, J. C. Linehan, R. S. Smith, B. D. Kay, B. Schmid, W. Shaw, M. Gutowski and T. Autrey, *Angew. Chem. Int. Ed*., 2005, **44**(23), 3578-3582.
14 Z. T. Xiong, C. K. Yong, G. T. Wu, P. Chen, W. Shaw, A. Karkamkar, T. Autrey, M. O. Jones, S. R. Johnson, P. P. Edwards and W. I. F. David, *Nat. Mater*., 2007, **7**, 138 - 141.
15 H. Wu, W. Zhou and T. Yildirim, *J. Am. Chem. Soc*., 2008, **130**(44), 14834-14839.
16 X. Kang, Z. Fang, L. Kong, H. Cheng, X. Yao, G. Lu and P. Wang, *Adv. Mater*, 2008, **20**(14), 2756-2759.
17 Z. T. Xiong, G. Wu, Y. S. Chua, J. Hu, T. He, W. Xu and P. Chen, *Energy Environ. Sci.,* 2008, **1**, 360-363
18 J. Spielmann, G. Jansen, H. Bandmann, S. Harder, *Angew. Chem. Int. Ed*, 2008, **47**(33), 6290-6295.
19 Z. T. Xiong, Y. S. Chua, G. T. Wu, W. L. Xu, P. Chen, W. Shaw, A. Karkamkar, J. Linehan, T. Smurthwaite and T. Autrey, *Chem. Commun.*, 2008, **43**, 5595-5597.
20 L. Li, X. Yao, C. Sun, A. Du, L. Cheng, Z. Zhu, C. Yu, J. Zou, S. C. Smith, P. Wang, H. M. Cheng, R. L. Frost and G. Q. Lu, *Adv. Funct. Mater.* , 2009, **19**(2), 265-271.
21 C. Z. Wu, G. T. Wu, Z. T. Xiong, W. I. F. David, K. R. Ryan, M. O. Jones, P. P. Edwards, H. L. Chu and P. Chen, *Inorg. Chem*., 2010, **49**, 4319–4323
22 C. Wu, G. Wu, Z. Xiong, X. Han, H. Chu, T. He and P. Chen, *Chem. Mater*., 2010, **22**(1), 3-5.
23 D. Y. Kim, N. J. Singh, H. M. Lee and K. S. Kim, *Chem-Eur. J*., 2009, **15**, 5598-5604
24 D. Y. Kim, H. M. Lee, J. Seo, S. K. Shin and K. S. Kim, *Phys. Chem. Chem. Phys*., 2010, **12**, 5446-5454.
25 S. A. Shevlin, B. Kerkeni and Z. X. Guo, *Phys. Chem. Chem. Phys*, **13** (17), 7649 - 7659.
26 A. T. Luedtke and T. Autrey, *Inorg. Chem*., 2010, **49**, 3905-3910
27 Y. S. Chua, P. Chen, G. Wu and Z. T. Xiong, *Chem. Commun.,* 2011, **47**, 5116-5129
28 G. L. Xia, X. B. Yu, Y. H. Guo, Z. Wu, C. Z. Yang, H. K. Liu and S. X. Dou, *Chem.–Eur. J*., 2010, **16**, 3763–3769.
29 K. R. Graham, T. Kemmitt and M. E. Bowden, *Energy Environ. Sci*., 2009, **2**, 706-710.
30 Y. S. Chua, G. T. Wu, Z. T. Xiong, T. He and P. Chen, *Chem. Mater*., 2009, **21**, 4899–4904
31 Y. S. Chua, G. T. Wu, Z. T. Xiong, A. Karkamkar, J. P. Guo, M. X. Jian, M. W. Wong, T. Autrey and P. Chen, *Chem. Commun*., 2010, **46**, 5752–5754
32 J. Luo, X. Kang, P. Wang, *Int. J. Hydrogen Energ*, 2013, **38**, 4648-4653
33 J. Chen, T. He, G. Wu, Z. Xiong, P. Chen, *Int. J. Hydrogen Energ*, 2013, **38**, 10944-10949
34 A. Bielecki and D. P. Burum, *J. Magn. Reson. Ser. A*, 1995. **116**, 215-220.
35 A. Staubitz, A. P. M. Robertson, and I. Manners, *Chem. Rev.* 2010, **110**, 4079–4124
36 D. J. Heldebrant, A. Karkamkar, J. C. Linehan and T. Autrey, *Energy Environ. Sci.* , 2008, **1**, 156-160
37 D. J. Wolstenholme, J. T. Titah , F. N. Che , K. T. Traboulsee , J. Flogeras , and G. S. McGrady. *J. Am. Chem. Soc.,* 2011, **133** (41), 16598–16604.
38 D. J. Wolstenholme, K. T. Traboulsee, Y. Hua, L. A. Calhoun and G. S. McGrady. *Chem. Commun*., 2012, **48**, 2597–2599.
39 D. J. Heldebrant, A. Karkamkar, N. J. Hess, M. Bowden, S. Rassat, F. Zheng, K. Rappe and T. Autrey, *Chem. Mater.,* 2008. **20**(16), 5332–5336.
40 C. X. Shang and Z. X. Guo, *J. Power Sources*, 2004, **129**(1), 73-80.
41 Y. H. Hu and E. Ruckenstein, *J. Phys. Chem. A*, 2003, 107(46), 9739-9741